LA-UR-90-1495

CONF-8910381--2

JUN 1 1990

LA-UR--90-1495

DE90 011956

TITLE: SYNTHETIC SPECTRA OF ACCRETION DISKS IN DQ HER BINARIES

AUTHOR(S): Christopher W. Mauche, LANL
Guy S. Miller, LANL
John C. Raymond, Harvard-Smithsonian Center for Astrophysics
Frederick K. Lamb, University of Illinois

SUBMITTED TO: 11th North American Workshop on CV's and LMXRV's

Synthetic Spectra of Accretion Disks in DQ Her Binaries

Christopher W. Mauche[1], Guy S. Miller[1], John C. Raymond[2], and Frederick K. Lamb[3]

[1]Space Astronomy and Astrophysics Group, Los Alamos National Laboratory
[2]Harvard-Smithsonian Center for Astrophysics
[3]Physics Department, University of Illinois at Urbana-Champaign

1 INTRODUCTION

Disk accretion by a strongly magnetic compact star differs fundamentally from disk accretion by a nonmagnetic star (see Lamb 1989). The interaction of the disk plasma with the stellar magnetic field drives electrical currents between the disk and the star. The resulting torque acts to bring the disk plasma and the star into corotation. At large radii, the gravitational and inertial stresses on the disk plasma greatly exceed the magnetic stress, and the angular velocity in the disk is nearly Keplerian. However, if the stellar magnetic field is strong enough, at some radius the rapidly increasing magnetic stress will dominate the other stresses, ending the Keplerian disk flow before it reaches the stellar surface. Here we call a star with such a strong magnetic field "strongly magnetic." Plasma approaching such a star leaves the disk near its inner edge and flows through the magnetosphere to the stellar surface, perhaps forming accretion columns above the magnetic poles.

The interaction of the disk plasma with the stellar magnetic field causes angular momentum to flow between the disk and the star. This flow is carried by the magnetic field, which is wound up by the shear between the relatively dense disk plasma, which orbits the star with the local Keplerian angular velocity, and the relatively tenuous magnetospheric plasma, which rotates with the angular velocity of the star. In a quasi steady flow, the pitch of the magnetic field is determined by competition between the shear, which tends to increase it, and dissipation of the electrical currents in the disk and magnetosphere, which tends to decrease it. Thus, an accretion disk around a strongly magnetic star differs in two important ways from a disk around a weakly magnetic star. First, the disk ends before it reaches the stellar surface. Second, the local heating rate within the disk is altered, both by changes in the rate of viscous energy dissipation caused by the angular momentum flows between the disk and the star and by the heating caused by dissipation of electrical currents flowing within the disk. Both the termination of the disk flow above the stellar surface and the changes in the local heating rate within the disk should profoundly affect the spectrum of the radiation emitted by the disk.

This effect should be observable in the optical and ultraviolet spectra of DQ Her stars, which have magnetic fields strong enough to end the disk flow before it reaches the stellar surface (Bianchini and Sabadin 1983; Wu *et al.* 1989). This expectation is supported by Verbunt's (1987) tabulation of the (de-reddened) ultraviolet spectral indices of a large sample of cataclysmic variable (CV) spectra from the *IUE* archive: the median wavelength spectral index (α, defined by $f_\lambda \propto \lambda^{-\alpha}$) of the 1460–2880 Å ultraviolet continua of DQ Her stars is 1.3, which is the lowest of *all* the tabulated groups of "high accretion rate" disk-accreting CVs. The median ultraviolet spectral index of all other groups is 2.0.

Here we explore the effect of the stellar magnetic field on the spectrum of the disk by comparing synthesized disk spectra to the observed ultraviolet spectrum of the well-studied DQ Her binary GK Per. We use the parameterized disk-magnetosphere interaction models of Miller and Lamb (1990; hereafter ML) to calculate the radius of the inner edge of the disk and the local heating rate within the disk as a function of radius. With appropriate choices of parameters, these models can describe the models of Ghosh and Lamb (1979*a*, *b*; hereafter GL) and Wang (1987). Once the local heating rate is determined, we assign an effective temperature to each of a series of disk annuli. The disk spectrum is then calculated by summing the flux contributed by each annulus, assuming that each annulus has the same spectrum as a main-sequence star with the assigned effective temperature.

2 CALCULATION OF DISK STRUCTURE

The inner edge of the Keplerian disk occurs where the magnetic stress becomes large enough to remove the angular momentum of the disk flow in a radial distance small compared to the distance to the accreting object (see Lamb 1989). Thus, the inner edge of the disk has nothing to do with pressure balance or the radial velocity in the disk, but is determined by the rate at which angular momentum is removed from the disk by the magnetic stress. The differential rate at which the magnetic stress removes angular momentum from the disk is

$$\frac{dN_{\rm mag}}{dr} = -r^2 B_\phi B_z \,, \tag{1}$$

where B_ϕ and B_z are respectively the azimuthal and vertical components of the magnetic field evaluated on a surface above the disk flow. ML show that the radius R_0 of the inner edge of the disk is close to the radius given implicitly by the relation

$$c_0 \dot{M} \Omega_K(R_0) = B_\phi(R_0) B_z(R_0) R_0 \,, \tag{2}$$

with $c_0 \approx 0.5$. Here $\dot{M}$ is the mass-accretion rate and $\Omega_K(r) = \sqrt{GM_*/r^3}$ is the local Keplerian angular velocity.

As noted in the Introduction, the disk is heated both by viscous energy dissipation and by dissipation of electrical currents. As is usual for thin disks, we assume that the energy dissipated at each radius is radiated locally. Then the differential luminosity of the disk at radius r is given by the radial derivatives of (1) the radial flux of gravitational potential and kinetic energy, (2) the radial energy flux carried by the viscous stress, and (3) the rate of energy injection by the magnetic stress. Thus,

$$\frac{dL}{dr} = \dot{M}\frac{d}{dr}\left(\Phi_{\rm grav} + \tfrac{1}{2}r^2\Omega_K^2\right) + \frac{d}{dr}(\Omega_K N_{\rm visc}) - \Omega_* \frac{dN_{\rm mag}}{dr} \tag{3a}$$

$$= -N_{\rm visc}\frac{d\Omega_K}{dr} - [\Omega_* - \Omega_K(r)]\,\frac{dN_{\rm mag}}{dr}, \tag{3b}$$

where $\Phi_{\rm grav}$ is the gravitational potential energy, $N_{\rm visc}$ is the angular momentum flux carried radially outward through the disk by the viscous stress, and Ω_* is the stellar angular velocity. In expression (3*b*), the various contributions to dL/dr have been rearranged to display explicitly the luminosity contributed by viscous energy dissipation and by dissipation of electrical currents.

The angular momentum flux carried by the viscous stress can be evaluated by using the fact that in a steady flow, the angular momentum entering and leaving any annulus of the disk must balance. Integrating the resulting differential equation from the inner edge of the disk, one obtains

$$N_{\rm visc}(r) = \dot{M}\left[r^2\Omega_K(r) - R_0^2\Omega_K(R_0)\right] - \int_{R_0}^{r} \frac{dN_{\rm mag}}{dr'}\,dr'\,. \tag{4}$$

The magnetic stress is determined by $B_\phi(r)$ and $B_z(r)$. ML consider two different prescriptions for $B_z(r)$, which give two sets of models. In the first set, $B_z(r)$ is assumed to be given by the z-component of an unscreened, dipolar stellar magnetic field, that is

$$B_z(r) = -\frac{\mu}{r^3}\,, \tag{5}$$

where μ is the dipole moment. In the second set of models, screening of the dipolar field by currents leaving the disk at R_0 is taken into account. As a result,

$$B_z(r) = -\frac{\mu}{r^3}\frac{B_z^2(R_0)}{B_z^2(R_0) + B_\phi^2(R_0)}\,. \tag{6}$$

In both sets of models, ML assume that (1) the interaction of the disk plasma with the magnetospheric field sweeps the field forward inside the disk corotation point (where the angular velocity of the disk plasma exceeds that of the star) and backward outside it (where the angular velocity is less than that of the star) and (2) the magnitude of the azimuthal component $B_\phi(r)$ is proportional to $B_z(r)$ times a power of r/R_A, where the Alfvén radius $R_A \equiv \mu^{4/7}(GM_*)^{-1/7}\dot{M}^{-2/7}$ is the usual length formed from μ, GM_*, and $\dot{M}$. Consistent with these assumptions, they write

$$B_\phi = g_0 B_z \left(\frac{|B_z| r^3}{\mu}\right)^{-4q/7}\left(\frac{r}{R_A}\right)^{q}\left|\frac{\Omega_* - \Omega_K}{\Omega_K}\right|^{p}\,\mathrm{sign}(\Omega_* - \Omega_K)\,. \tag{7}$$

The factor $|B_z|r^3/\mu$ is equal to unity in the models that assume an unscreened poloidal field. In the models that include screening, this factor effectively scales the radius

R_A, which is defined in terms of the unscreened field, bringing it into accord with the local poloidal field strength.

These models allow one to study the observational consequences of various radial variations of the magnetic pitch by considering different exponents p and q and different values of the "coupling constant" g_0. They can also be used to explore some of the effects of screening of the poloidal magnetic field.

3 CALCULATION OF DISK SPECTRA

We assume that the differential luminosity of the disk around a strongly magnetic star is given by equation (3). For comparison, we assume that the differential luminosity of the disk around a weakly magnetic star is given by

$$\frac{dL}{dr} = \frac{3}{2}\frac{GM_*\dot{M}}{r^2}\left[1-\left(\frac{R_*}{r}\right)^{1/2}\right], \tag{8}$$

which is appropriate if the star is rotating slowly. Once the differential luminosity is determined, we compute the effective temperature using the relation

$$\sigma T_{\rm eff}^4 \equiv \frac{1}{4\pi r}\frac{dL}{dr}, \tag{9}$$

where σ is the Stefan-Boltzmann constant.

We assume that each annulus of the disk radiates the same spectrum as a main-sequence star with the effective temperature given by equation (9). The spectra have been chosen from a library of 46 de-reddened main-sequence stellar spectra ranging in temperature from 3,100 K to 47,000 K for spectral types M5 to O5. The vacuum ultraviolet ($\lambda\lambda \sim$ 1150–3200 Å) spectra in the library were taken from the *IUE* spectral atlas of Wu *et al.* (1984) while the optical ($\lambda\lambda \sim$ 3500–7500 Å) spectra were taken from the KPNO library of Jacoby, Hunter, and Christian (1984).

These elemental spectra have been synthesized into a disk spectrum using a computer code developed by S. Kenyon (Cannizzo and Kenyon 1987; Kenyon 1989). This code is similar to the one developed by Wade (1984). Like Wade, we assume that the disk flow is everywhere optically thick, physically thin, and steady. We approximate the continuous variation of the disk temperature with radius by a grid of temperatures chosen to match the temperatures of library spectra. An approximate spectrum of the complete disk is then constructed by summing the library spectra that correspond to the temperatures in the grid, weighting each one by the area of the corresponding annulus. In order to compare the spectra of disks around strongly and weakly magnetic stars, we synthesize the spectra of both types of disks for every choice of parameters.

4 RESULTS

For the sake of brevity, we consider here only the well-studied DQ Her binary GK Per; a more complete discussion will be published elsewhere. The "observables" for this source are: *IUE* spectra SWP 13497 and LWP 10143 and FES measurements of GK Per in outburst, the distance (d = 470 pc), the inclination ($i < 73°$), and the reddening ($E_{B-V} = 0.3$ mag), which we used to produce Figure 1; the orbital period ($P_{\rm orb} = 47.9$ hr) and the mass ratio ($q = M_*/M_{\rm sec} = 3.6$), which imply an accretion disk outer radius $R_d \approx 2 \times 10^{11}$ cm; and the mass ($M_* = 0.9\,{\rm M}_\odot$) and spin period ($P_{\rm spin} = 351$ s) of the white dwarf, which imply that the corotation radius is $R_c = (GM_*/\Omega_*^2)^{1/3} = 7.5 \times 10^9$ cm. We focus our attention on outburst spectra because they are least affected by emission from the secondary, the white dwarf, and the hot spot where the accretion stream strikes the outer disk. In comparing our synthesized disk spectra to observed spectra, we assume that contributions to the observed spectra from the boundary layer at the inner disk edge and from the accretion columns and stellar surface are negligible.

In order to define a model with a weakly magnetic white dwarf, one must specify M_*, R_*, R_d, and $\dot{M}$. If the white dwarf is strongly magnetic and rotating at its equilibrium spin rate, one must also specify $P_{\rm spin}$ and g_0, p, and q [cf. eq. (7)]. Finally, if the white dwarf is strongly magnetic but is not rotating at its equilibrium spin rate, one must also specify μ. In the two latter types of models, the white dwarf spin rate can be characterized by the fastness parameter $\omega_s \equiv \Omega_*/\Omega_K(R_0)$.

The fastness parameter at which the torque on the star vanishes is called the critical fastness and is denoted ω_c. Although the fastness of GK Per in outburst is not necessarily the equilibrium fastness, as illustrative examples we restrict ourselves to the consideration of models for which $\omega_s = \omega_c$. ML found that an unscreened model with $g_0 = 5$, $p = 1.0$, and $q = 1.2$ (which implies $\omega_c = 0.28$ and $R_0 = 0.42\,R_c$) was consistent with the $\dot{P}(L)$ relation found by Parmar *et al.* (1989) and power spectrum data obtained by Angelini, Stella, and Parmar (1989) from observations of EXO 2030+375. (However, these parameters are subject to large uncertainties because the orbital elements of this source are poorly known.) We shall refer to this choice of parameters as strongly magnetic white dwarf model A. The ML parameters that reproduce the magnetic stresses of the GL physical model are $p = 0.5$ and $q = 0.86$, which give $\omega_c = 0.74$. We refer to this choice of parameters as model B. The value of ω_c originally quoted by GL for their model was 0.35; this lower value was the result of an algebraic error (see Lamb 1989). Using $\omega_c = 0.74$, the radius of the inner edge of the disk is $R_0 = 0.82\,R_c$ rather than $R_0 = 0.50\,R_c$.

Figure 2 compares the predictions of three different models of the accretion disk in GK Per: the weakly magnetic white dwarf model and the strongly magnetic white dwarf models A and B. All three models assume a mass-accretion rate $\dot{M} = 10^{-7.5}\,{\rm M}_\odot\,{\rm yr}^{-1}$. The effects of injection and extraction of energy by the magnetic stress are clearly seen in both models A and B, for which the magnetic field strengths are found to be 3.3 MG and 7.5 MG, respectively. The magnetic stress extracts energy from the disk in the interval between R_0 and R_c but injects energy into the disk at radii larger than R_c. Because model A extends to smaller radii than model B, its maximum temperature is higher. However, the maximum temperatures

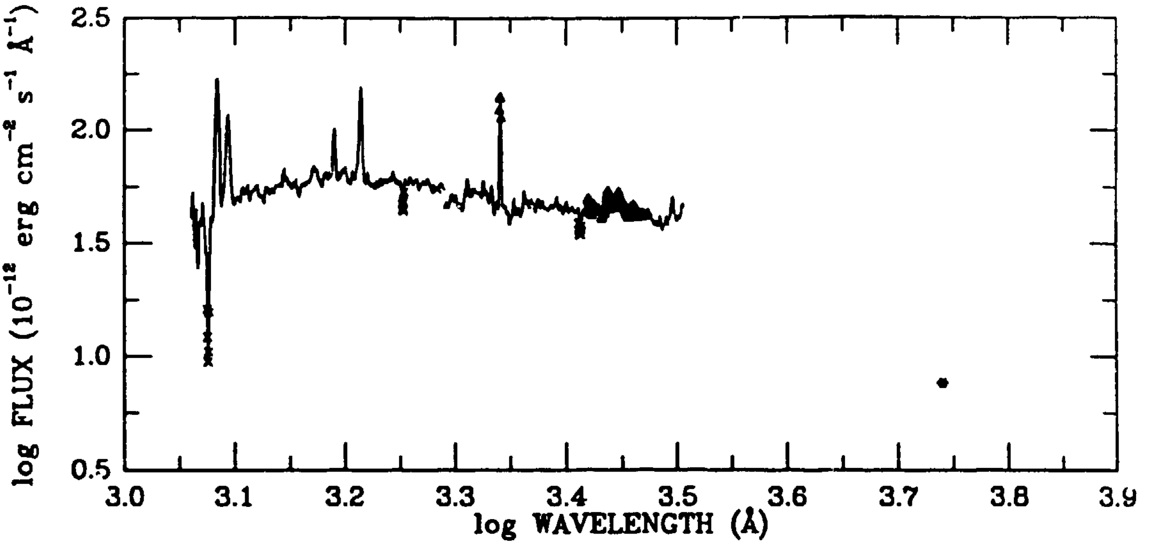

Fig. 1—The dereddened optical through ultraviolet outburst spectral distribution of GK Per, scaled to a distance of 100 pc and corrected for its inclination ($f_\lambda \leftarrow f_\lambda \times (470/100)^2/\frac{2}{5}(1+\frac{3}{2}\cos 70°)$). The spectral index $\alpha \equiv -\log(f_{1460}/f_{2880})/\log(1460/2880)$ is ≈ 1.0, although the spectrum is poorly fit by a power law. The various geometric symbols represent various data quality flags: extrapolated ITF pixels (*triangles*), saturated pixels (*filled triangle*), and reseaux (*crosses*).

of both strongly magnetic white dwarf models are significantly less than the maximum temperature of the weakly magnetic white dwarf model. The peak temperature of model A is $\approx$ 50,000 K, compared to the $\approx$ 125,000 K peak temperature of the weakly magnetic white dwarf model; the peak temperature of model B is $\approx$ 20,000 K, less than half that of model A. According to Figure 1, the flux distribution of GK Per during outburst peaks at $\approx$ 1600 Å, implying a maximum temperature in the disk of $\sim$ 18,000 K. Thus, the reduction of the peak temperature that occurs when the white dwarf is strongly magnetic is comparable in size to the reduction needed to explain the spectrum during outburst.

Turning to the resulting disk spectra, the 1460–2880 Å ultraviolet spectral index changes from 2.5 to 2.2 to 2.0 as one goes from the weakly magnetic white dwarf disk to the strongly magnetic model A disk and then to the model B disk. Although the spectra of all three models match the observed spectrum poorly (cf. Fig. 1), this decrease of $\approx$ 0.5 in the ultraviolet spectral index is comparable to the difference of $\sim$ 0.7 between the ultraviolet spectral indices of Verbunt's (1987) sample of *IUE* spectra of DQ Her binaries and the spectral indices of all other "high accretion rate" CVs, indicating that the magnitude of the effect is correct. The spectral index of the Balmer continuum in stars is greater than the spectral index of a blackbody with the same temperature because radiative transfer processes redistribute flux from shortward of the Balmer and Lyman edges to longward of them. As a result, disk

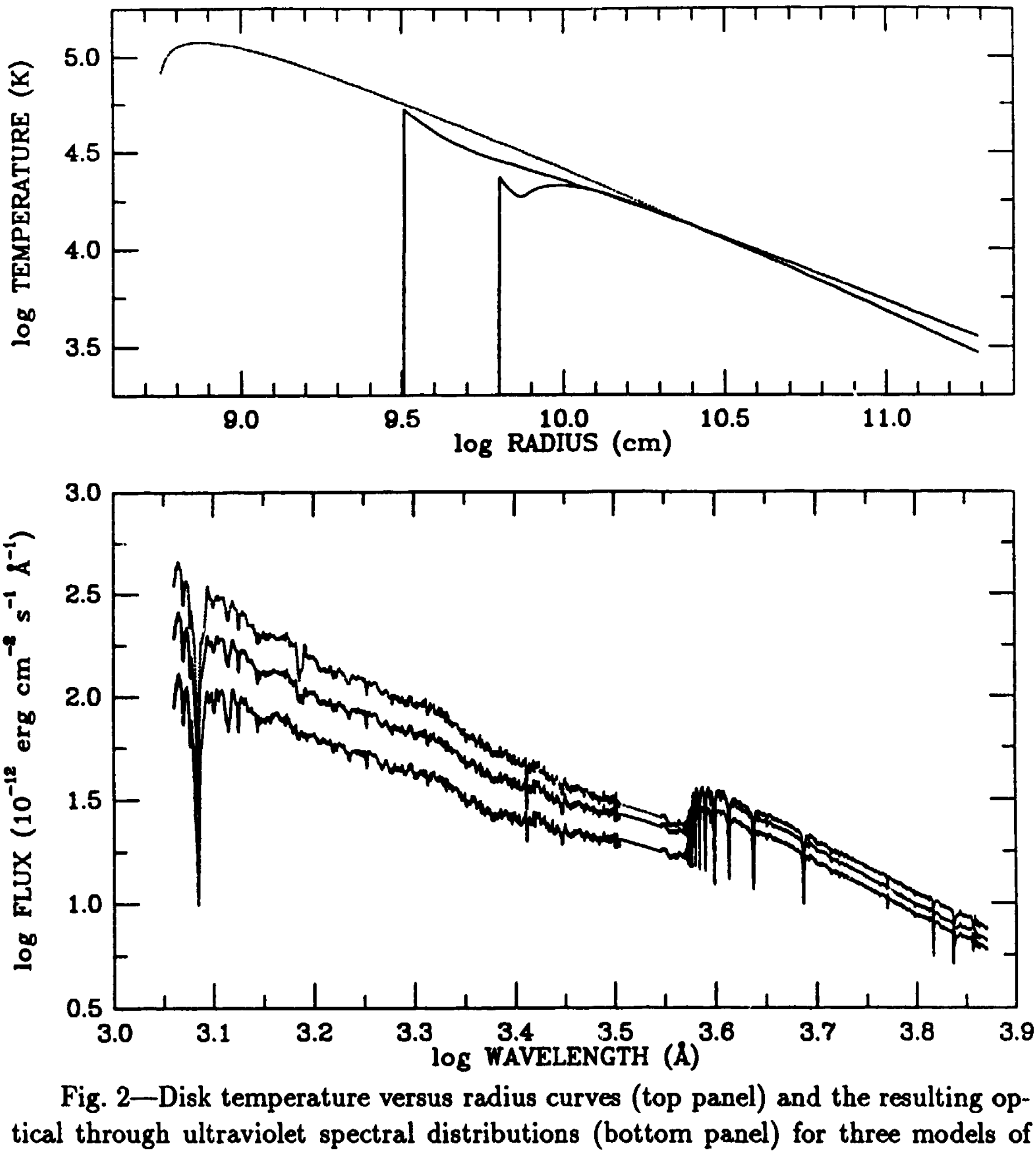

Fig. 2—Disk temperature versus radius curves (top panel) and the resulting optical through ultraviolet spectral distributions (bottom panel) for three models of GK Per: (1) the weakly magnetic white dwarf model (*upper, dotted curves*), (2) the strongly magnetic white dwarf model *A* (*middle, solid curves*), and (3) the strongly magnetic white dwarf model *B* (*lower, solid curves*).

spectra synthesized from blackbody spectra will be flatter than the spectra shown in Figure 2. The construction of synthetic disk spectra based on blackbody spectra is currently under way.

In summary, we find that it is possible to reproduce both the level and spectral index of the observed optical through ultraviolet spectrum of GK Per in outburst for certain choices of the parameters in the ML description of disk accretion by a strongly

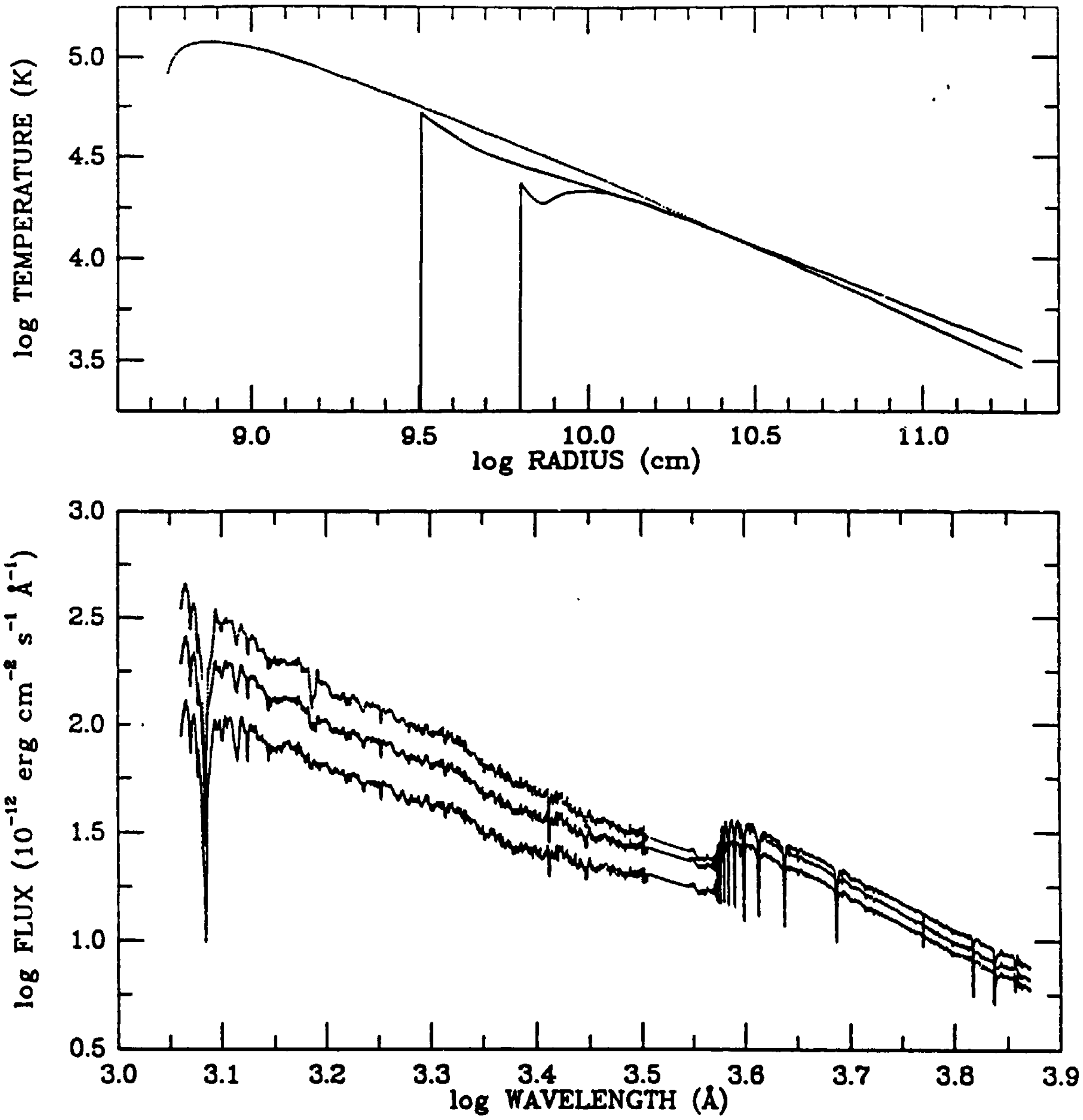

Fig. 2—Disk temperature versus radius curves (top panel) and the resulting optical through ultraviolet spectral distributions (bottom panel) for three models of GK Per: (1) the weakly magnetic white dwarf model (*upper, dotted curves*), (2) the strongly magnetic white dwarf model A (*middle, solid curves*), and (3) the strongly magnetic white dwarf model B (*lower, solid curves*).

spectra synthesized from blackbody spectra will be flatter than the spectra shown in Figure 2. The construction of synthetic disk spectra based on blackbody spectra is currently under way.

In summary, we find that it is possible to reproduce both the level and spectral index of the observed optical through ultraviolet spectrum of GK Per in outburst for certain choices of the parameters in the ML description of disk accretion by a strongly magnetic compact star. This result indicates that synthetic accretion disk spectra can be used to constrain models of the accretion disks in DQ Her binaries and to provide insights into the nature of the disk-magnetosphere interaction in such systems. The knowledge gained in this way will also help to improve our understanding of disk accretion by other types of strongly magnetic compact stars.

This research was supported in part by NSF grant PHY 86-00377 and NASA grant NAGW 1583 at the University of Illinois and by the U.S. Department of Energy.

REFERENCES

Angelini, L., Stella, L., and Parmar, A. N. 1989, *Ap. J.*, **346**, 906.
Bianchini, A., and Sabadin, F. 1983, *Astr. Ap.*, **125**, 112.
Cannizzo, J. K., and Kenyon, S. J. 1987, *Ap. J.*, **320**, 319.
Ghosh, P., and Lamb, F. K. 1979*a*, *Ap. J.*, **232**, 259, GL.
Ghosh, P., and Lamb, F. K. 1979*b*, *Ap. J.*, **234**, 296, GL.
Jacoby, G. H., Hunter, D. A., and Christian, C. A. 1984, *Ap. J. Suppl.*, **56**, 257.
Kenyon, S. J. 1989, private communication.
Lamb, F. K. 1989, in *Timing Neutron Stars*, ed. H. Ögelman and E. P. J. van den Heuvel (Dordrecht: Kluwer), p. 649.
Miller, G. S., and Lamb, F. K. 1990, in preparation, ML.
Parmar, A. N., White, N. E., Stella, L., Izzo, C., and Ferri, P. 1989, *Ap. J.*, **338**, 359.
Verbunt, F. 1987, *Astr. Ap. Suppl.*, **71**, 339.
Wade, R. A. 1984, *M. N. R. A. S.*, **208**, 381.
Wang, Y.-M. 1987, *Astr. Ap.*, **183**, 257.
Wu, C.-C., *et al.* 1984, *IUE NASA Newsletter*, No. 22.
Wu, C.-C., *et al.* 1989, *Ap. J.*, **339**, 443.